

The Role of Coronal Hole and Active Region Boundaries in Solar Wind Formation

Louise K. Harra

*UCL-Mullard Space Science Laboratory, Holmbury St Mary, Dorking, Surrey,
RH5 6NT, UK*

Abstract. *Hinode* observations have provided a new view of outflows from the Sun. These have been focussed in particular on flows emanating from the edges of active regions. These flows are long lasting and seem to exist to some extent in every active region. The flows measured have values ranging between tens of km s^{-1} and 200 km s^{-1} . Various explanations have been put forward to explain these flows including reconnection, waves, and compression. Outflows have also been observed in coronal holes and this review will discuss those as well as the interaction of coronal holes with active regions. Although outflowing plasma has been observed in all regions of the Sun from quiet Sun to active regions, it is not clear how much of this plasma contributes to the solar wind. I will discuss various attempts to prove that the outflowing plasma forms part of the solar wind.

1. Introduction

The slow solar wind is more dynamic and has speeds of a few hundred km s^{-1} whereas the fast solar wind is steady with speeds of 800 km s^{-1} . The fast solar wind originates from regions where the magnetic fields lines are open. The slow solar wind is more complicated with several different scenarios to explain its origins. These include reconnection between open coronal hole and closed helmet streamer magnetic field (e.g., Crooker et al. 2004), reconnection between open flux and closed flux which displaces the open field lines (e.g., Fisk 2003), and reconnection between closed loops associated with active regions and nearby open flux. Irrespective of which scenario you choose to explain the slow solar wind, it is clear that the boundaries of both coronal holes and active regions are important in the formations and development of both the slow and fast solar wind.

McComas et al. (2008) shows the change in the behaviour of the solar corona during the first Ulysses orbit (during a solar minimum period), the second Ulysses orbit (during a solar maximum), and the final Ulysses orbit (during solar minimum again) (see Figure 1). The first orbit shows a 'classic' solar minimum with the Sun taking the form of a clear dipole with the streamer belt at the equator. The heliospheric current sheet tilt is very low. The second orbit shows a 'classic' solar maximum period where the streamer belt is chaotic and reaches high latitudes, with the polar coronal holes becoming less clear. The heliospheric current sheet tilt was high. The final orbit is the most recent solar minimum at the start of solar cycle 24. During this period the streamer belt was not lying along the equator and the heliospheric current tilt is higher than the previous solar minimum. The interactions between open and closed field drive

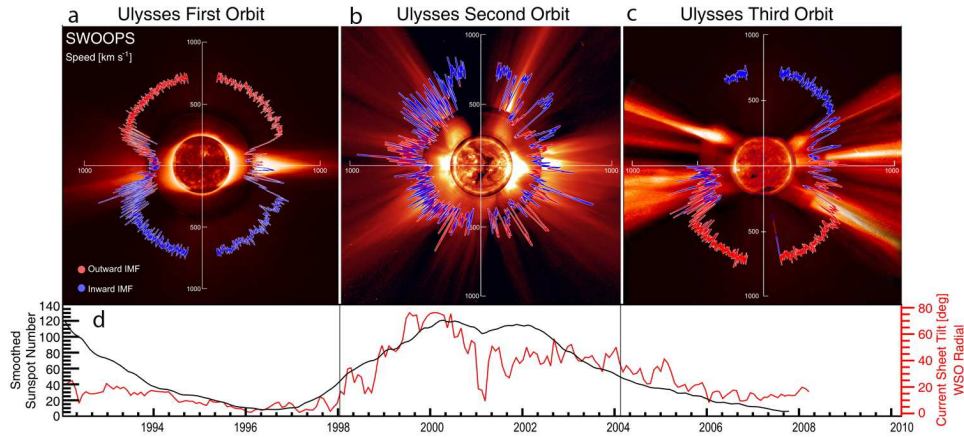


Figure 1. *Top:* Polar plots of the solar wind speed from three orbits obtained by the Ulysses spacecraft. *Bottom:* Sunspot number and heliospheric current sheet tilt during the same time period. From McComas et al. (2008). Copyright 2008 American Geophysical Union.

the changes observed in the solar cycle. In this review we will discuss some potential sources of the slow and fast solar wind from active region, coronal hole, and quiet Sun boundaries and discuss whether these sources do actually form part of the solar wind.

2. Coronal Holes, Their Boundaries, Their Formation and Larger Scale Impact

The fast solar wind is known to emanate from coronal holes where the magnetic field lines are predominantly open to interplanetary space. Polar coronal holes are in some senses simpler than equatorial coronal holes as they have fewer interactions with surroundings than equatorial coronal holes that lie in the activity belt. Hence we begin by describing polar coronal holes. Strong magnetic field patches have been discovered in the polar coronal holes. These have been compared to the quiet Sun magnetic field by Ito et al. (2010) and they found that the average area and the total magnetic flux of the kilo-Gauss magnetic concentrations in the polar region is larger than those of the quiet Sun. Tian et al. (2010) studied the temperature behaviour of the outflows with EIS in a polar coronal hole and found that the outflow appears to start in the transition region. Figure 2 illustrates outflowing plasma in different part of the solar atmosphere. The outflow becomes more prominent with increasing temperature. Significant outflows appear as small patches in the transition region, and these patches merge together as the temperature of the plasma increases. This is consistent with the concept of the solar wind being guided by expanding magnetic funnels as described by Tu et al. (2005) where the plasma is accelerated above 5 Mm.

Equatorial coronal holes, on the other hand, have the potential to interact with the more 'active' Sun. The formation of equatorial coronal holes and their interaction with their surroundings is important in terms of understanding the solar cycle. Karachik et al. (2010) have studied a number of cases where equatorial coronal holes have formed during active region decay. As active regions decay, the leading and lagging magnetic polarities usually exhibit different dissipation rates. This causes an increase in the magnetic flux imbalance as the region decays, and a coronal hole will

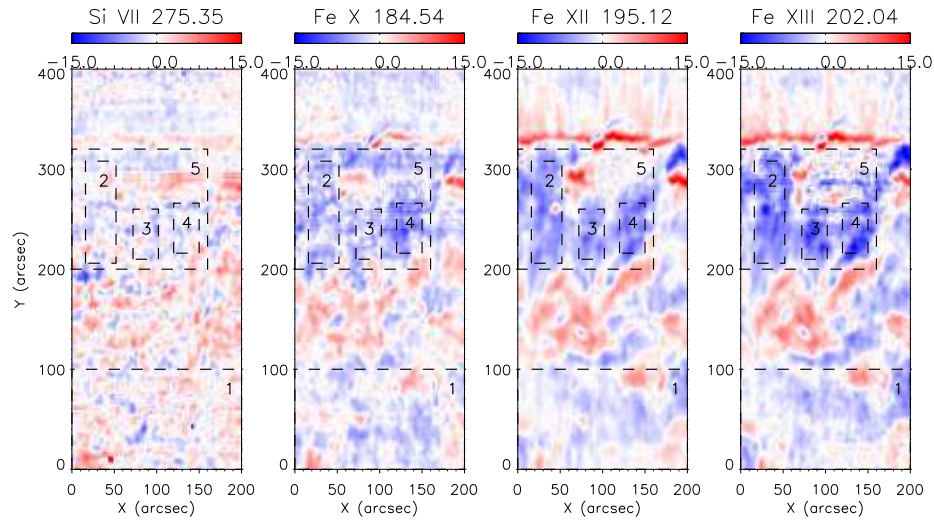


Figure 2. Doppler velocity maps of the north polar coronal hole from EIS, with blue showing blue-shifted plasma and red showing red-shifted plasma. The Doppler velocity range is $\pm 15 \text{ km s}^{-1}$. From Tian et al. (2010). Reproduced by permission of AAS.

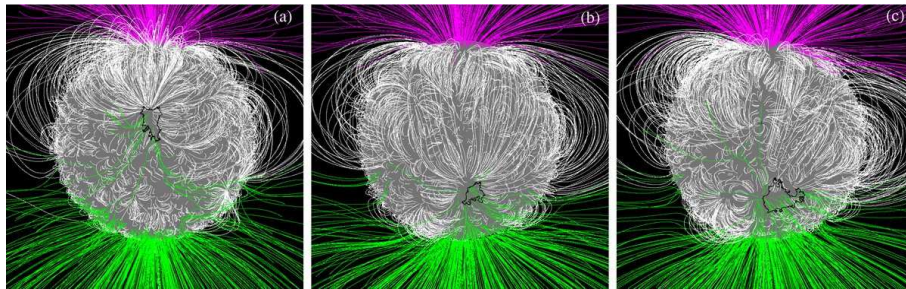


Figure 3. Magnetic field extrapolations highlighting the linkage between the three equatorial coronal holes and the north polar coronal hole during the recent solar minimum period. From Karachik et al. (2010), reproduced by permission of AAS.

form in the place where the most compact polarity existed in the active region. Figure 3 shows magnetic field extrapolations of three examples of coronal holes formed followed active region decay. All the regions studied were observed during the end of solar cycle 23 and beginning of solar cycle 24. The equatorial coronal holes had their magnetic field ending in the north polar coronal hole, regardless of which hemisphere the coronal hole was located. This indicates the flux imbalance between the north and south coronal hole during this unusual solar minimum. The behaviour of the coronal holes is suggestive of the change from toroidal to poloidal magnetic field that is required to transition from one solar cycle to another, as is described by the Babcock-Leighton model.

We have discussed equatorial and polar coronal holes—but is there a difference in their characteristics quantitatively? Raju (2009) analysed the Doppler velocities and line widths in both coronal holes at the poles and equator and compared these values

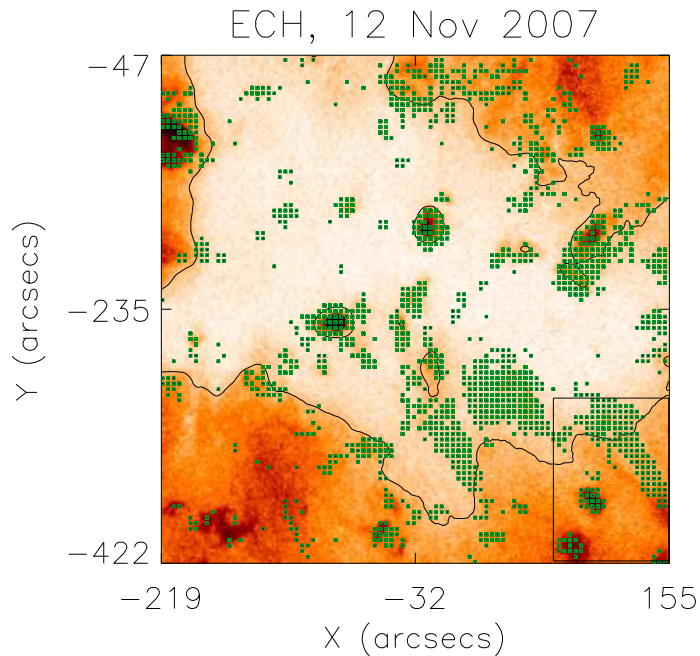


Figure 4. An equatorial coronal hole observed by TRACE. The coronal hole boundary is highlighted in black. Positions of identified brightenings are overlaid in green. From Subramanian et al. (2010). Reproduced with permission ©ESO.

with quiet Sun measurements. They found that the coronal holes have larger blue-shifts and increased line widths than quiet Sun regions, which would be expected as the magnetic field lines are expected to be dominantly open in coronal holes, allowing faster outflow. It was also found that polar coronal holes have larger line width relative to an equatorial coronal hole. It is also possible that the reason for this is that the equatorial coronal holes are surrounded by closed magnetic field and will have interactions with this.

Subramanian et al. (2010) studied the interactions between equatorial coronal holes and the surrounding quiet Sun. Figure 4 shows an example where the positions of brightenings are overlaid. The brightenings were each analysed to search for evidence of outflow such as expanding loops or collimated flows. Only 30% of the brightenings in the quiet Sun showed evidence of outflowing plasma whereas 70% of the brightenings in the coronal hole showed outflowing plasma. The brightenings are often concentrated at the coronal hole-quiet Sun boundary, the cause of which is likely to be interchange reconnection between open and closed magnetic field lines. This process will result in strong plasma outflows that can form part of the solar wind.

Coronal holes, as well as interacting with quiet Sun and other coronal holes, can also interact with active regions. Yokoyama & Masuda (2010) have studied this interaction using Yohkoh data to analyse how large-scale trans-equatorial loops are formed.

As a new active region emerges it interacts with the polar coronal hole through interchange reconnection. The new loops that are formed due to this reconnection cause the coronal hole boundary to slowly retreat as the active region continues to emerge.

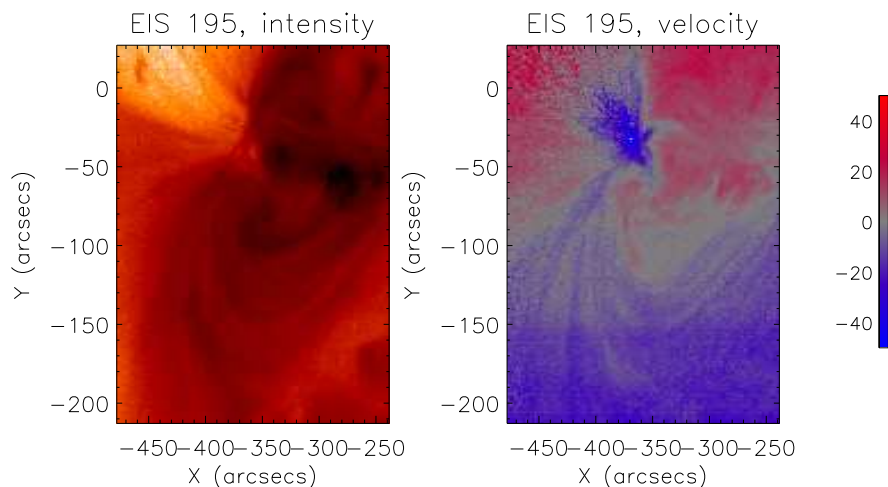


Figure 5. *Left:* Intensity image of an active region observed by *Hinode* EIS in the Fe XII coronal emission line. *Right:* Doppler velocity data, showing strong outflows as blue.

Yokoyama & Masuda (2010) believe that this boundary interaction is important in the formation of trans-equatorial loops (TEs). The magnetic field between the coronal hole and active region begins as semi-open. As these fields interact with the emerging active region, they form large-scale loop structures. The bright TEL appears through chromospheric evaporation process which is accompanied by the eruption of the loop structure.

The large scale structure of the atmosphere is driven to some extent by coronal holes and their interaction with the surroundings. In the next section we will divert our attention to active regions and their boundaries with quiet Sun and coronal holes.

3. Boundaries of Active Regions with Coronal Holes and Quiet Sun

It is clear that active regions can provide an input to the slow solar wind, but it is not obvious exactly what the source of this is. Active regions are observed to continuously expand (e.g., Uchida et al. 1992). *Hinode* observations are now allowing us to consistently measure outflow at the edges of active regions (Figure 5). This outflow is observed as steady streams of outflow in imaging data (see Sakao et al. 2007). Using density measurements they estimated that $\approx 25\%$ of the slow solar wind could come from such outflowing regions. Spectroscopic data from EIS shows that there are strong outflows persistently at the edges of the active region (e.g., Harra et al. 2008) with main line profile showing bulk shifts of up to 50 km s^{-1} . Additional blue-shifted components have been also been observed as show in Figure 6.

There are a number of explanations that have been put forward to explain the outflows. Turbulence at the footpoints was initially suggested by Hara et al. (2008), who found a clear relationship between the enhanced line widths observed and the Doppler velocities which suggests unresolved flows are seen. Harra et al. (2008) used magnetic field extrapolations and found that the region of strong outflow was a site of

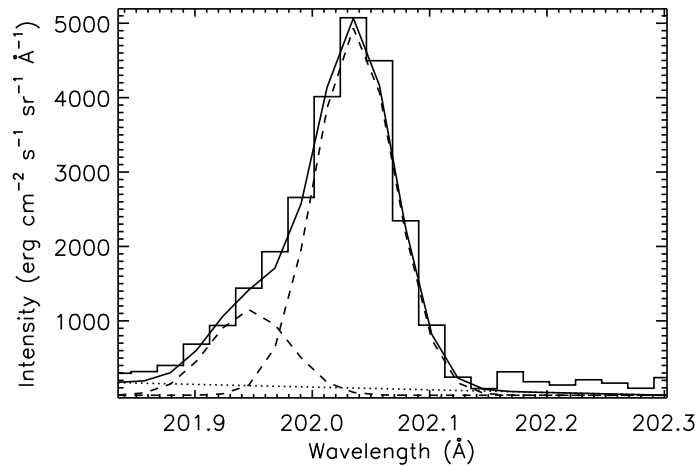


Figure 6. The spectral line profile of the Fe XIII emission line observed with EIS at the edge of an active region. There is a very clear blue component. A double Gaussian profile is used to fit both components. From Bryans et al. (2010). Reproduced by permission of AAS.

reconnection with another remote bipole which would allow field lines to be opened. Murray et al. (2010) found through 2.5D magnetohydrodynamic simulations of a flux tube emerging into a coronal hole that the flows could be replicated. Reactionary forces are generated in the coronal hole magnetic field as the active region loops expand, which accelerates the plasma. Baker et al. (2009) determined the location of quasi-separatrix layers (QSLs), which are the regions that show strong gradients in the magnetic connectivity. The strongest QSLs are found to be at the edges of the active regions where the outflows are most enhanced. This shows that the outflow regions are potential locations of magnetic reconnection.

The outflows described above are seen in the corona. The unresolved outflows have been analysed by using a blue-red asymmetry method which measures the relative intensities in the red and blue wing of a line profile. This is a way to measure the weak but strongly blue-shifted component in the line profile. De Pontieu et al. (2009) studied the chromospheric link to the outflows by looking at this blue-red asymmetry through the atmosphere and found this behaviour to be consistent throughout the atmosphere. Indeed the patches of strong blue-red asymmetry seem consistently related to chromospheric brightenings as seen in Figure 7. Their model to explain the outflows intimately relates them to chromospheric spicules (see Figure 8). They estimate that only a few percent of spicules need to be heated to coronal temperatures to heat the corona.

The chromospheric linkage is not just seen in the line profile asymmetry but also in the intermittency. He et al. (2010) studied the dynamic behaviour of outflows in different temperature regimes. They found that the outflows occur 17 times within 5 hours, and are seen both in X-rays and the EUV with speeds exceeding 200 km s^{-1} . They found chromospheric jets at the root of each strand that was producing the outflows.

The triggering mechanism for the outflows is as yet not clear. Harra et al. (2010) have analysed an active region during additional flux emergence into one of the bipoles. The new flux emergence triggers a reconfiguration of the active region, as would be

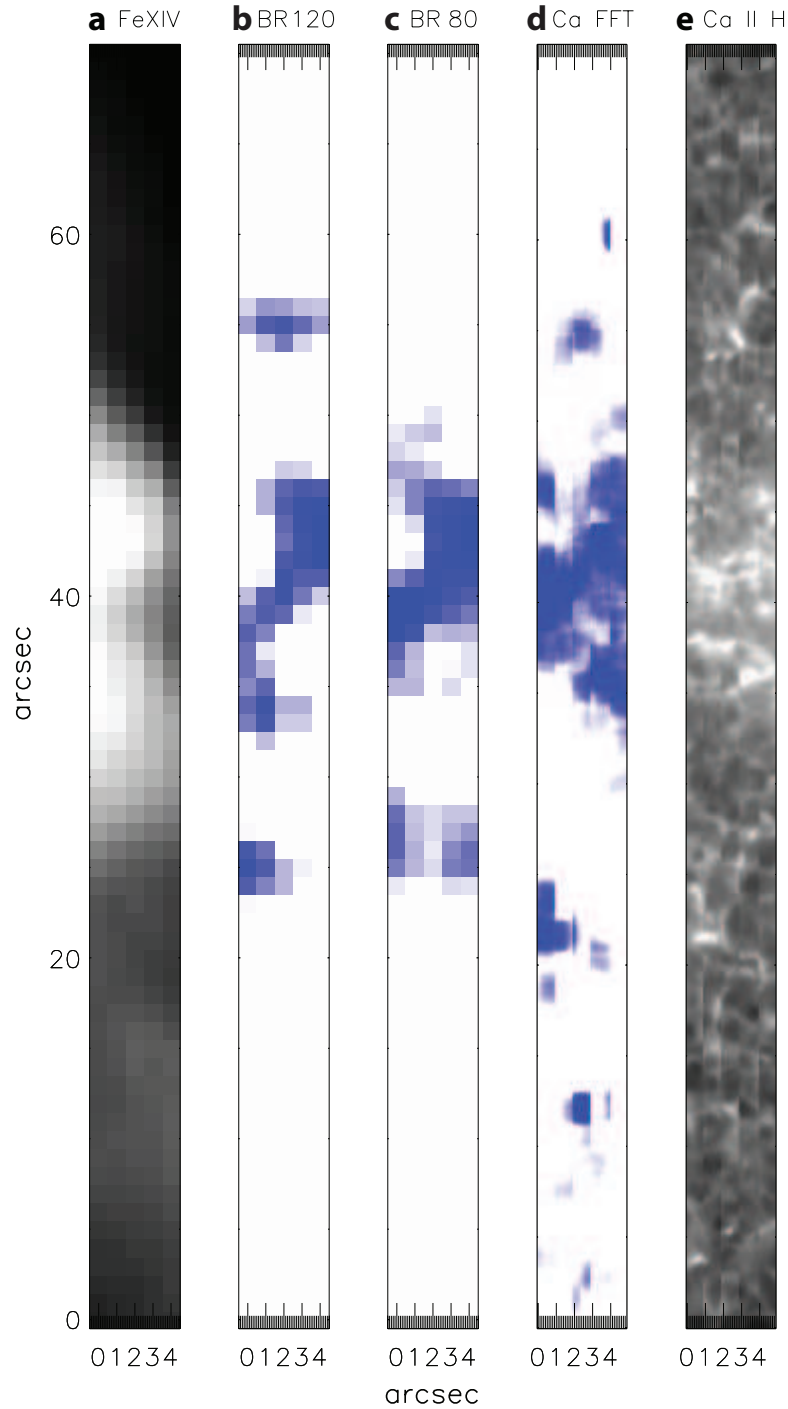


Figure 7. (a) Intensity of the Fe XIV line. (b) Blue-red asymmetry centred on 120 km s^{-1} . (c) Blue-red asymmetry centred on 80 km s^{-1} , (d) Chromospheric data from Ca II H passed through a temporal high-pass Fourier filtering to show the upper chromospheric dynamics only. (e) Ca II H intensity data. From De Pontieu et al. (2009). Reproduced by permission of AAS.

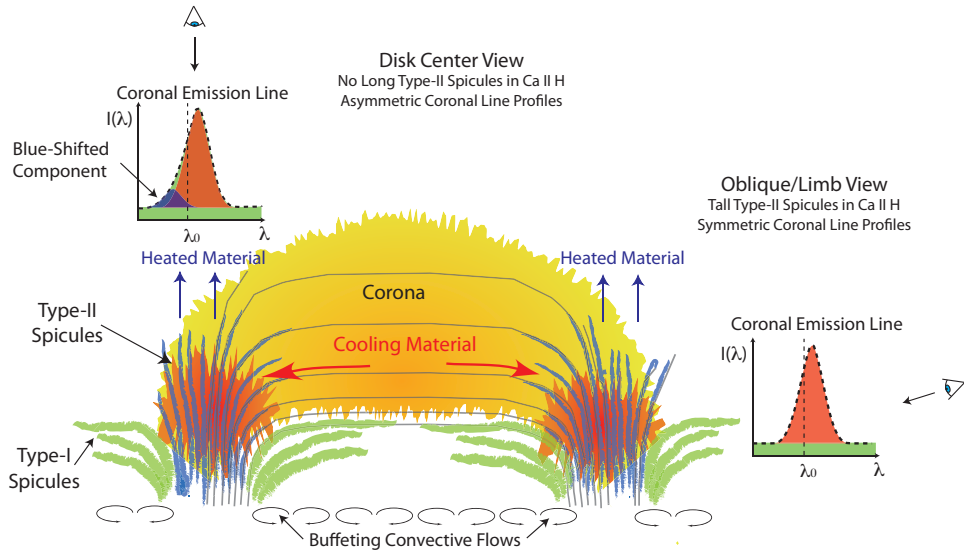


Figure 8. A cartoon describing the possibility for the spicular material to be heated to coronal temperature. This would show as a strong but weak blue shifted component in the corona. From De Pontieu et al. (2009). Reproduced by permission of AAS.

expected. One of the responses to the new flux emergence was that enhanced outflowing material appeared. This was not just on the side of the new bipole that was most favourable for reconnection, but also appeared strongly as a clear 'ring' of enhanced Doppler velocities of the east side of the active region which did not have favourable magnetic field orientation for reconnection. This enhanced Doppler velocity lasted for many hours (see Figure 9). We know that flux emergence exists on all scales from granular scales to active region scales, and this could also drive the outflows.

In this section we concentrated on recent results of outflowing plasma in active regions. The active regions studied have different neighbours, be it coronal holes, another active region or quiet Sun. These interactions will affect the contribution to the solar wind. A systematic statistical study is needed to progress understanding further.

4. Does Any of the Outflowing Plasma Form Part of the Solar Wind?

Although outflows are seen persistently at the edges of active regions, and it has been suggested that they could form part of the solar wind, it is not trivial to prove this. Del Zanna et al. (2010) have studied noise storms, which are seen at higher altitudes in the corona and indicate a beam of electrons. They found that the radio noise storms are persistently seen and are located above the active region outflows. They argue for a reconnection scenario that is pressure driven and continues because of the expansion of the active region. The outflows are then linked to large-scale open separatrix field lines and the radio noise storms, and map the electron beams propagating in the high corona above the active regions. Since the densities of the active region and nearby coronal hole in their example are so different, after reconnection occurs, the section belonging

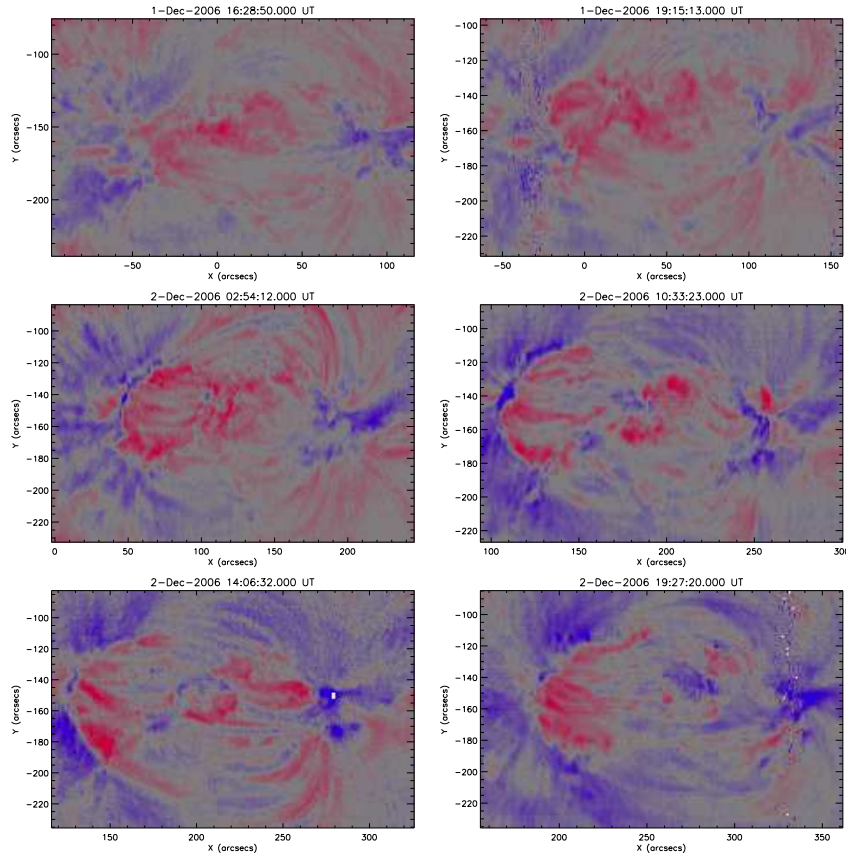


Figure 9. A time series of Doppler velocity images in an active region derived from the Fe XIII emission line. New flux emergence occurred in the west part of the active region. From Harra et al. (2010).

to the former active region will have a much higher density than the coronal hole. This will lead to the launch of a rarefaction wave.

To track the outflow beyond the electron beams observed in the radio wave emission, in-situ data from the ACE spacecraft needs to be used. He et al. (2010) analysed the ACE data for the period during February 2007 and combined it with solar data. This example was for an active region close to a coronal hole, so the coronal hole is easily seen in the ACE data as a high speed stream (see Figure 10). The solar wind stream emanating from the active region flows has an intermediate velocity.

A longer term analysis was carried out to study the solar wind related to active region outflows over a Carrington rotation. Figure 11 illustrates the back-mapped solar wind and the composition data measured from ACE along with the EUV image of the corona from the EUV Imager on board STEREO (EUVI). Seven regions are labeled on the synoptic image. Each of these was observed by EIS on *Hinode* and the approximate location of the strongest outflow highlighted in the figure. The solar wind speeds related to the active regions are intermediate speeds, with those active regions located next to a coronal hole (S1, S3, and S5/S6) showing the most significant increase in wind speed. The ion composition shows a confusing picture with values for the 'active re-

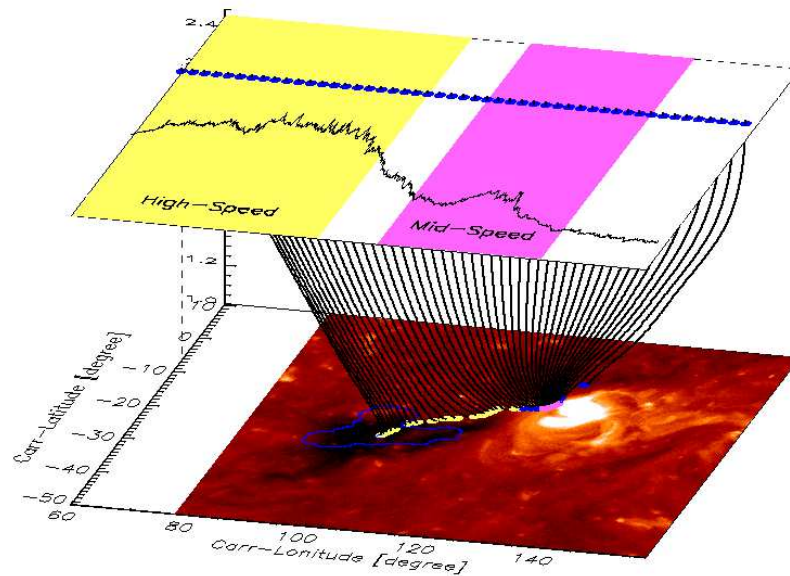


Figure 10. The lower images shows the coronal data with the blue contour outlining the coronal hole detected by Kitt Peak. The magnetic field is extrapolated to 2.5 solar radii. The upper image shows the solar wind speed measured at 1 AU by ACE. From He et al. (2010). Reproduced with permission ©ESO.

gion' wind ranging from similar to coronal hole composition to similar to active region composition.

In the in-situ data the slow wind plasma typically shows a greater proportion of elements of low First Ionisation Potential (< 10 eV) compared to fast wind (e.g., Schwadron et al. 1999). This is interpreted as indicating a different source for slow wind, in which electron temperatures are higher, and that slow wind originates on closed loops. Ko et al. (2006) found from analysis of the Sun at 1.64 solar radii that the source of the slow solar wind seemed to be predominantly the coronal hole and active region boundary. Another means to determine whether the outflowing plasma seen from active regions on the Sun actually forms part of the slow solar wind is to study the composition at the solar disk. Brooks & Warren (2011) have studied the relative abundance of Si (a low FIP element) and S (a high FIP element) for one active region over a period of 5 days. They found that Si is enhanced over S by a factor of 3–4 which is consistent with in situ measurements. This demonstrates that the plasma flowing from active regions does have the same composition as that measured in the slow solar wind. This was however carried out for one active region. The interaction of an active region with nearby coronal holes and other factors may affect the composition and dynamics of the outflowing plasma. Longer term studies need to be carried out in order to understand the complex interactions.

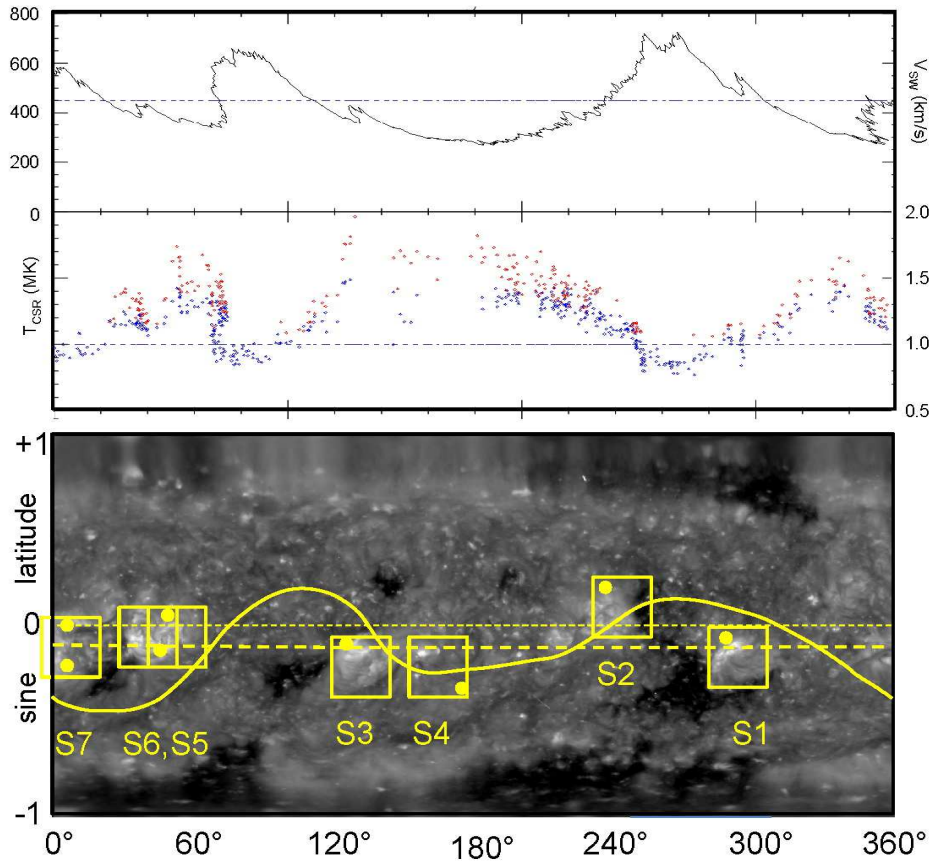


Figure 11. *Top:* Wind speed measured by ACE which has been back-mapped. *Middle:* Oxygen composition in blue. *Bottom:* EUVI synoptic map with the locations of the different regions studied highlighted by yellow boxes and identified by a label. Courtesy A. Fazakerley.

5. Conclusions

Outflowing plasma is seen in all regions of the Sun on the disk—from coronal holes, quiet Sun, active region edges, and the interaction between these three regions. *Hinode* can observe the dynamics of these regions in great detail. In the future more systematic and longer term studies are needed to unravel the complexity of the interactions of one type of phenomena on the Sun to another. In particular consistent linkage to in-situ data is critical. This will be of particular interest as the solar cycle slowly progresses to a maximum, and during the imminent period of polarity reversal.

Acknowledgments. *Hinode* is a Japanese mission developed and launched by ISAS/JAXA, collaborating with NAOJ as a domestic partner, NASA and STFC (UK) as international partners. Scientific operation of the *Hinode* mission is conducted by the *Hinode* science team organized at ISAS/JAXA. This team mainly consists of scientists from institutes in the partner countries. Support for the post-launch operation

is provided by JAXA and NAOJ (Japan), STFC (UK), NASA (USA), ESA, and NSC (Norway).

References

- Baker, D., van Driel-Gesztelyi, L., Mandrini, C. H., Démoulin, P., & Murray, M. J. 2009, *ApJ*, 705, 926
- Brooks, D. H., & Warren, H. P. 2011, *ApJ*, 727, L13
- Crooker, N. U., Huang, C.-L., Lamassa, S. M., Larson, D. E., Kahler, S. W., & Spence, H. E. 2004, *J. Geophys. Res. (Space Physics)*, 109, 3107
- De Pontieu, B., McIntosh, S. W., Hansteen, V. H., & Schrijver, C. J. 2009, *ApJ*, 701, L1
- Fisk, L. A. 2003, *J. Geophys. Res. (Space Physics)*, 108, 1157
- Hara, H., Watanabe, T., Harra, L. K., Culhane, J. L., Young, P. R., Mariska, J. T., & Doschek, G. A. 2008, *ApJ*, 678, L67
- Harra, L. K., Magara, T., Hara, H., Tsuneta, S., Okamoto, T. J., & Wallace, A. J. 2010, *Solar Phys.*, 263, 105
- Harra, L. K., Sakao, T., Mandrini, C. H., Hara, H., Imada, S., Young, P. R., van Driel-Gesztelyi, L., & Baker, D. 2008, *ApJ*, 676, L147
- He, J.-S., Marsch, E., Tu, C.-Y., Guo, L.-J., & Tian, H. 2010, *A&A*, 516, A14
- Ito, H., Tsuneta, S., Shiota, D., Tokumaru, M., & Fujiki, K. 2010, *ApJ*, 719, 131
- Karachik, N. V., Pevtsov, A. A., & Abramenko, V. I. 2010, *ApJ*, 714, 1672
- Ko, Y.-K., Raymond, J. C., Zurbuchen, T. H., Riley, P., Raines, J. M., & Strachan, L. 2006, *ApJ*, 646, 1275
- McComas, D. J., Ebert, R. W., Elliott, H. A., Goldstein, B. E., Gosling, J. T., Schwadron, N. A., & Skoug, R. M. 2008, *Geophys. Res. L.*, 351, 18103
- Murray, M. J., Baker, D., van Driel-Gesztelyi, L., & Sun, J. 2010, *Solar Phys.*, 261, 253
- Raju, K. P. 2009, *Solar Phys.*, 255, 119
- Sakao, T., Kano, R., Narukage, N., Kotoku, J., Bando, T., DeLuca, E. E., Lundquist, L. L., Tsuneta, S., Harra, L. K., Katsukawa, Y., Kubo, M., Hara, H., Matsuzaki, K., Shimojo, M., Bookbinder, J. A., Golub, L., Korreck, K. E., Su, Y., Shibasaki, K., Shimizu, T., & Nakatani, I. 2007, *Science*, 318, 1585
- Schwadron, N. A., Fisk, L. A., & Zurbuchen, T. H. 1999, *ApJ*, 521, 859
- Subramanian, S., Madjarska, M. S., & Doyle, J. G. 2010, *A&A*, 516, A50
- Tian, H., Tu, C., Marsch, E., He, J., & Kamio, S. 2010, *ApJ*, 709, L88
- Tu, C.-Y., Zhou, C., Marsch, E., Xia, L.-D., Zhao, L., Wang, J.-X., & Wilhelm, K. 2005, *Science*, 308, 519
- Uchida, Y., McAllister, A., Strong, K. T., Ogawara, Y., Shimizu, T., Matsumoto, R., & Hudson, H. S. 1992, *PASJ*, 44, L155
- Yokoyama, M., & Masuda, S. 2010, *Solar Phys.*, 263, 135